The Influence of the Side-Wall on the Flow around the Circular Cylinder with Tangential Injection of Air

by

Fumio YOSHINO* and Ryoji WAKA*

(Received October 20, 1975)

The experimental investigation has been carried out to inquire into the cause of the three-dimensionality of the flow around the circular cylinder with tangential injection of air. It was found by means of the oil-flow method that a strong vortex is shed from the surface of the cylinder near a side-wall and that seems to be the cause of the three-dimensionality.

1 Introduction

We have carried out the experiment about the flow around a circular cylinder with tangential injection of air for some years, and many knotty problems resulted from the experiment[1]. Some of them were those of the influence of R_e, θ_J and C_μ on the transition of boundary layers of the external flow, the influence of R_e and AR on the relation of C_{pb} to θ_{USP}, the structure of the slot, induced drag at the center of span and so on.

However we took the most interest in the existence of the induced drag even at the center of the span, because, in the experiment of this kind, the flow around the cylinder is in general regarded as two-dimensional. Then we carried out the experiment[2] to require into the cause for this induced drag under the condition that AR and C_μ were varied while R_e and θ_J were kept constant. As a result of this experiment, the strong vortex was found in the wake of the cylinder near the side-wall (see Fig. 1). It is thought that this vortex seems to be generated by the secondary flow of the boundary layer on the side-wall and is concerned with the three-dimensionality of the flow.

In this report, we present the experimental result obtained so far.

* Department of Mechanical Engineering

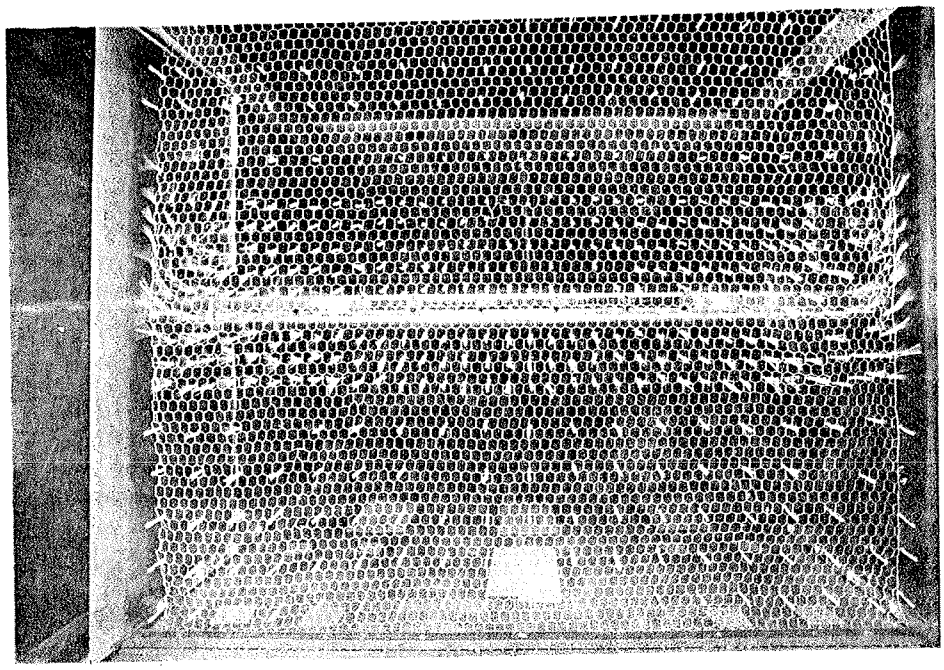

Fig. 1 The vortex in the wake visualized by means of the tufts method. ($X/D = 4.6$, $R_e = 0.5\times10^5$, $AR=8$ **and** $C_\mu = 0.22$)

2 Nomenclatures

X = Distance from the center of the cylinder along the tunnel axis downstream ;

Y_W = Distance from the side-wall in spanwise direction ;

Z = Perpendicular distance from the horizontal plane passing through the central axis of the cylinder ;

D = Diameter of the cylinder ;

b_0 = Width of the slot ;

θ = Angle measured clockwise from the leading edge ;

θ_J = Angular position of the slot measured from the top of the cylinder downstream ;

θ_{USP} & θ_{LSP} = Angular positions of the upper- and the lower-separation points on the cylinder, respectively ;

P_S = Static-pressure on the surface of the cylinder ;

P_∞ = Static-pressure in the wind tunnel ;

C_p = Static-pressure coefficient $\left(= \dfrac{P_S - P_\infty}{1/2\ \rho\ U_\infty^2} \right)$;

C_{pb} = Base-pressure coefficient ;

C_{ls} = Sectional lift coefficient;

C_μ = Momentum coefficient of jet $\left(= \dfrac{M \quad b_0}{1/2 \ \rho \ U_\infty^2 \ D} \right)$;

M = Momentum of jet at the outlet of the slot;

R_e = Reynolds number $\left(= \dfrac{U_\infty \ D}{\nu} \right)$;

U_∞ = Tunnel speed;

AR = Aspect ratio of the cylinder;

ρ & ν = Density and kinematic viscosity coefficients of air in the wind tunnel, respectively.

3 Experimental installment and method

The experimental apparatus was the same that we had used before[2]. The experiment was carried out under the condition that R_e and θ_J were constant, that is, 2.1×10^5 and 0°, respectively.

The measurements of the static-pressure on the cylinder were made at three aspect ratios, 4, 6 and 8, by properly varying C_μ from 0 to about 0.3. However the observations of the flow and the other measurement described below were made at only one aspect ratio, 8, and in some narrow range of C_μ from 0 to about 0.25, but, in this case, R_e and θ_J were remained unchanged.

The streamline on the side-wall was visualized by using the tufts method. Moreover the streamlines on the cylinder and the side-wall were visualized by using the oil-flow method. Finally we measured the static-pressure in the symmetric plane including the center of the span in it. It was measured by means of the disk-static head with round edge. This disk has dimensions of 15 *mm* in diameter and 0.8 *mm* in thickness and is drilled the static-pressure-hole of 0.5 *mm* in diameter at the center of it. In this measurement, R_e was 1.5×10^5, since the vibration of the disk was too large to measure accurate static-pressure.

4 Results and Discussion

The results of this experiment are represented in graphs and pictures.

Fig. 2 shows the separation lines of the flow in the spanwise direction. In this figure, the symbols indicate the separation points obtained from the static-pressure distribution on the cylinder and the lines indicate the separation lines obtained from the oil-flow method (see Fig. 6). The larger the C_μ is, the later the upper-separation is, however the lower-separation is scarcely influenced by C_μ. When $C_\mu = 0$, the

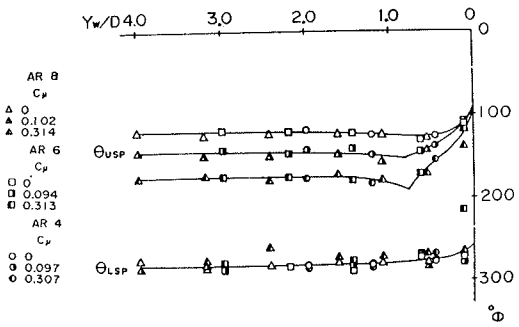

Fig. 2 The separation lines on the cylinder.

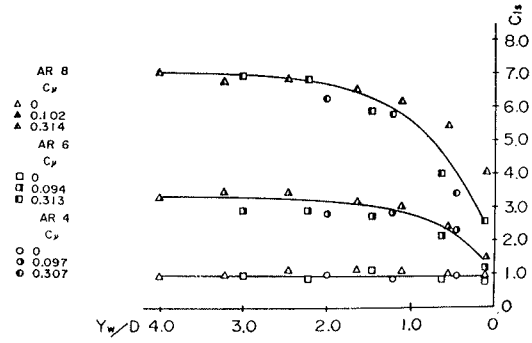

Fig. 3 The spanwise distribution of C_{ls}.

upper- and lower-separation lines are almost straight except very near the side-wall. On the other hand, when $C_\mu > 0$, the upper-separation line is varied in spanwise direction so much ; the separation point begins to move gradually toward downstream from somewhere about $Y_W/D = 1.5$ and reaches the farthest point at about $Y_W/D = 0.7$, after that it retreats rapidly as approaching to the side-wall.

Fig. 3 shows the spanwise distribution of C_{ls}. C_{ls} is almost constant over the whole span when $C_\mu = 0$. When $C_\mu > 0$, C_{ls} is also almost constant as far as about $Y_W/D \geqq 1.5$, however it decreases rapidly near the side-wall. Moreover the larger the C_μ is, the larger the rate of decrease of C_{ls} near the side-wall is.

Fig. 4 shows the spanwise distribution of C_{pb}. When $C_\mu = 0$, C_{pb} is almost constant over the whole span. However when $C_\mu > 0$, C_{pb} is varied so much ; it begins to decrease rapidly from somewhere about $Y_W/D = 1.5$ and reaches the minimum value at about $Y_W/D = 0.6$, then it increases rapidly as approaching to the side-wall.

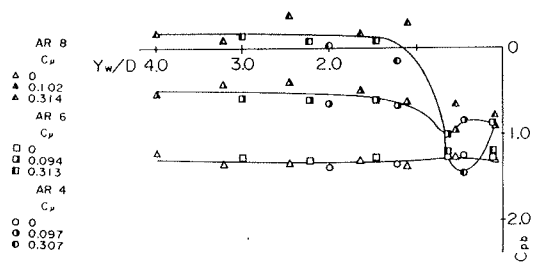

Fig. 4 The spanwise distribution of C_{pb}.

It is found from these figures that the flow around the cylinder may be considered approximately two-dimensional in the region from the center of the span to somewhere about $Y_W = 1.5$, if induced velocity is ignored, since the characteristic values like C_{pb}, θ_{USP} and C_{ls} of the flow in this region are almost the same as those at the center of the span. The influence of the side-wall strongly appears in particular near the side-wall, that is, in the region from somewhere about $Y_W/D = 1.5$ to the side-wall. However it is thought that the flow patterns near the side-wall are qualitatively alike and is independent of AR when $C_\mu > 0$ or, in other words, is a function of the distance only from the side-wall, since all the variations of the

characteristic values near the side-wall occur within the same range from the wall irrespective to *AR*.

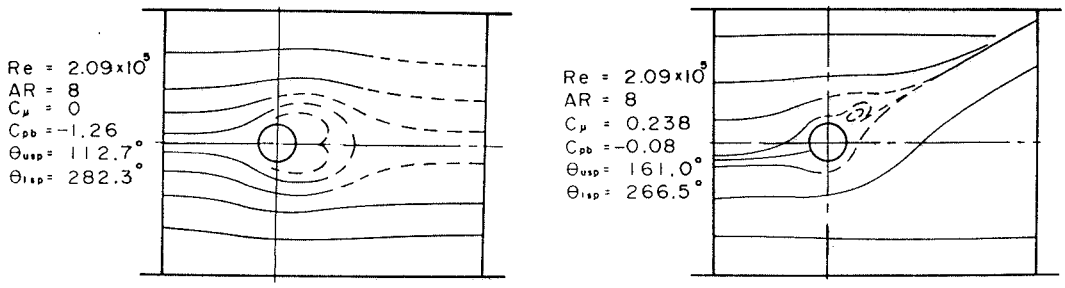

Fig. 5 The streamlines on the side-wall.

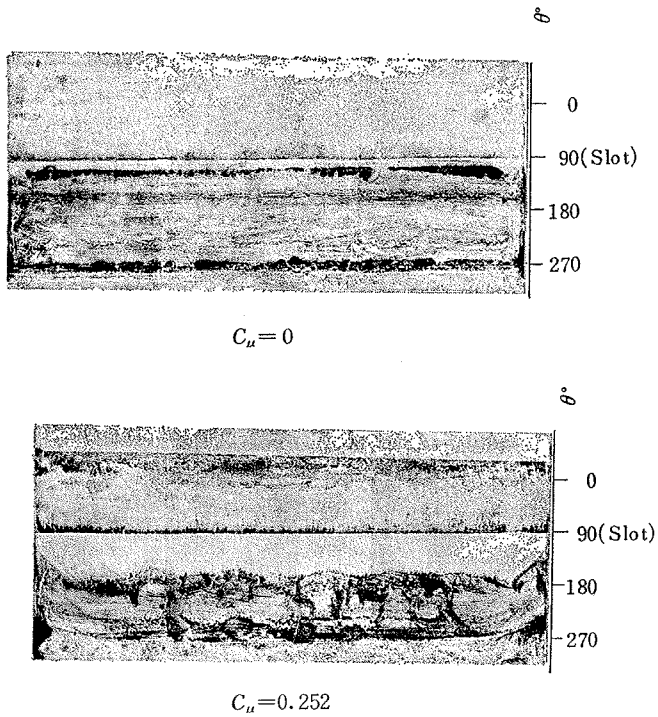

Fig. 6 The streamlines on the cylinder visualized by means of the oil-flow method. ($R_e = 2.1\times10^5$)

Fig. 5, Fig. 6 and Fig. 7 show the streamlines on the side-wall, on the cylinder and the static-pressure distributions in the symmetric plane at the center of the span, respectively. Fig. 5 is obtained from tufts method (solid lines) and oil-flow method (dotted lines, see Fig. 8). Fig. 9 shows the equal-static-pressure lines around the cylinder obtained from Fig. 7. When $C_\mu = 0$, it is found from these figures

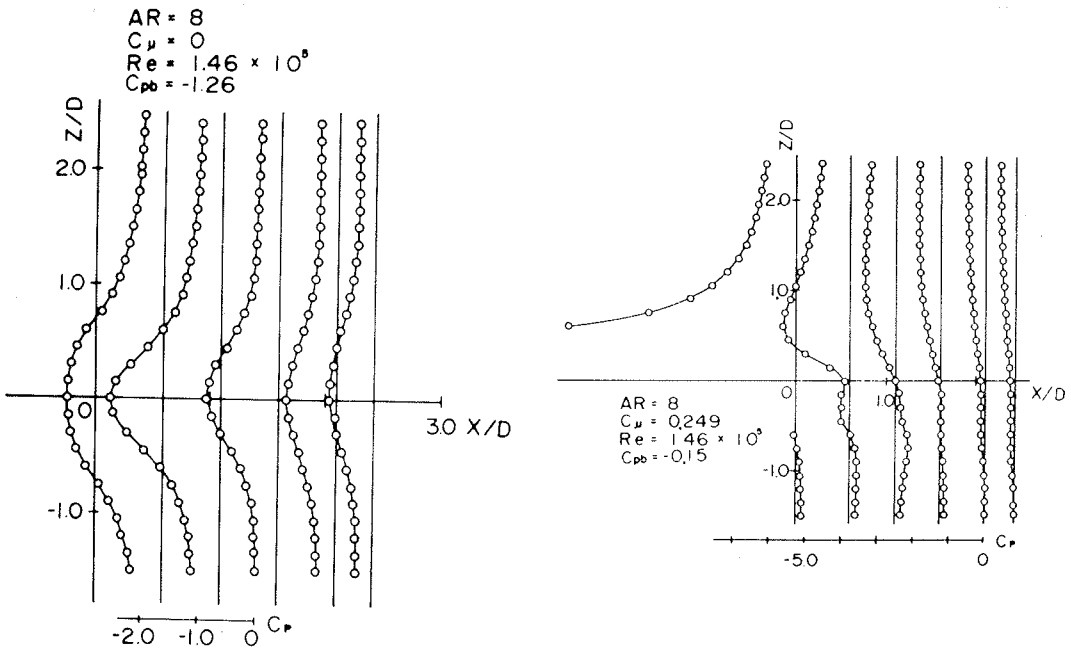

Fig. 7 The static-pressure distributions around the cylinder in the symmetric plane.

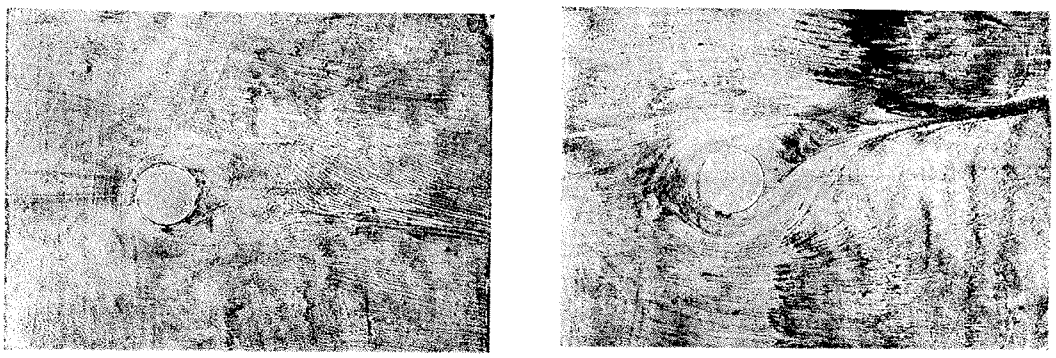

$C_\mu = 0$ $C_\mu = 0.249$

Fig. 8 The streamlines on the side-wall visualized by means of the oil-flow method. ($R_e = 2.1 \times 10^5$)

that the flow is almost symmetric with respect to X-axis and the influence of the side-wall on the flow is not seen so clear. When $C_\mu > 0$, however, the static-pressure of the flow is lower at the upper-side than that at the lower-side of the cylinder (see Fig. 9). This indicates that circulation around the cylinder arises, so that aerodynamical force acts on the cylinder. On the other hand, the streamlines on the side-wall direct upwards behind the cylinder. This may be thought as follows ;

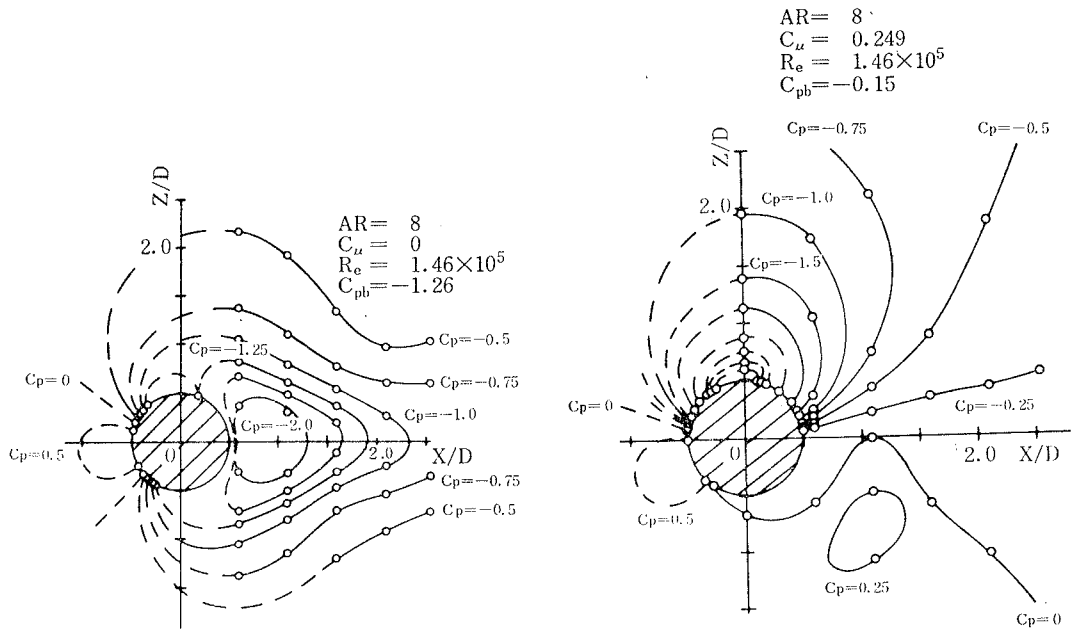

Fig. 9 The equal-static-pressure lines around the cylinder in the symmetric plane.

the static-pressure gradient around the cylinder is not symmetric and the static-pressure on the upper-side is lower than that on the lower-side. Therefore the secondary flow ought to be directed upwards behind the cylinder (see Fig. 8).

Moreover a strong vortex appears on the cylinder near the side-wall (see Fig. 6) and it is shed from the surface of the cylinder. The central position of this vortex which rotates counterclockwise is about Y_W/D = 0.6 regardless of AR and it nearly coincides with the position of the vortex observed in the wake (see Fig. 1). And this vortex seems to have a certain relation to the secondary flow on the side-wall.

Concludingly, it is thought that the variation of the characteristic values near the side-wall are caused by this strong vortex, which means that those variations are the function of the distance from the side-wall and not of AR.

5 Conclusion

(1) The strong vortex exists on the surface of and in the wake of the cylinder when $C_\mu > 0$ and it is shed from there downstream.

(2) The flow around the cylinder is considered to be nearly two-dimensional in the region from the center of the span to $Y_W/D \fallingdotseq 1.5$, but it is necessary to take

induced velocity into account.

(3) All the characteristic values are functions of the distance from the side-wall, not of AR, and the variations of those are related to the vortex mentioned in (1).

Reference

1) Furuya and Yoshino, Bull. JSME, 18-123 (1975-9), 1002.

2) Furuya, Yoshino and Waka, Preprint of Bulletin of JSME and JSPE, (in Japanese), (Showa 49-11), 7.